

Two-dimensional tunnel bifurcations with dissipation

A. K. Aringazin*

*Department of Theoretical Physics, Institute for Basic Research,
Eurasian National University, Astana 473021, Kazakhstan[†]*

Yuri Dahnovsky[‡]

*Department of Physics and Astronomy, P.O. Box 3905,
University of Wyoming, Laramie, WY 82071, USA*

V. D. Krevchik,[§] M. B. Semenov,[¶] and V. A. Veremyev[§]

Department of Physics, Penza State University, 40 Krasnaya St., Penza 440017, Russia

A. A. Ovchinnikov

Joint Institute of Chemical Physics, Kosygin Street 4, 117334 Moscow, Russia

K. Yamamoto

Research Institute of International Medical Center of Japan, Tokyo, Japan

(Dated: August 20, 2003)

Two-particle tunneling in synchronous and asynchronous regimes is studied in the framework of dissipative quantum tunneling. We show that the use of the proposed model is justified by a comparison with realistic potential energy surfaces of porphyrin and experimental dependence of the reaction rate on temperature. The critical temperature T_c corresponding to a bifurcation of the underbarrier trajectory is determined. The effect of a heat bath local mode on the probability of two-dimensional tunneling transfer is also investigated. At certain values of the parameters, the degeneracy of antiparallel tunneling trajectories is important. Thus, four, six, twelve, etc., pairs of the trajectories should be taken into account (a cascade of bifurcations). For the parallel particle tunneling the bifurcation resembles phase transition of a first kind, while for the antiparallel transfer it behaves as second order phase transition. The proposed theory allows for the explanation of experimental data on quantum fluctuations in two-proton tunneling in porphyrins near the critical temperature.

PACS numbers: 03.65 Xp, 03.65 Sq, 31.15 Gy, 31.15 Kb, 73.40 Gk, 82.20 Xr

I. INTRODUCTION

Quantum tunneling dynamics of a particle interacting with a heat bath is one of the important problems of modern condensed matter physics [1]–[30]. The interest to this problem is related to studies in low-temperature superconductive tunnel junctions [5, 6, 9], a dissipative quantum tunneling in crystals [13], and low-temperature chemical reactions [1, 24, 25, 26, 27, 28, 29, 30]. In low dimensional systems an effective mass approximation often fails. Thus, quantum tunneling with dissipation becomes an important tool in the description of electron transfer [3, 13]. In many physical processes tunneling of *two* particles occurs. For example, Semenov and Dakhnovskii [28, 29] found the bistability of the tunneling trajectories in a two-proton transfer. Later, Benderskii and co-workers extended their investigations to different two-dimensional potentials [30]. Some features of the two-dimensional tunneling dynamics were studied in interacting Josephson junctions [6].

Another example of two-particle tunneling is a two-proton transfer in porphyrin systems [27, 28, 29]. Porphyrins are important molecules in Biology [31] and a new area of Electronics – molecular wires and devices [32]. There are experimental data [24, 25, 26, 33] that clearly indicate that a tunneling instability occurs at some critical temperature. Such a behavior in the rate constant demonstrates the existence of bifurcations in two-dimensional underbarrier

*Electronic address: aringazin@mail.kz; Also at Kazakhstan Division, Moscow State University, Moscow 119899, Russia.

[†]URL: <http://www.emu.kz>

[‡]Electronic address: yurid@uwyo.edu

[§]Electronic address: physics@diamond.stup.ac.ru

[¶]Electronic address: physics@diamond.stup.ac.ru; Also at Institute for Basic Research, P.O. Box 1577, Palm Harbor, FL 34682, USA.

trajectories. Apparently, this effect requires a thorough investigation when the protons interact with a thermal bath.

The effect of cleavage in the temperature dependence of the current for two-dimensional systems of interacting Josephson junctions was identified in Ref. [6]. However, there was no experimental confirmation of this effect. In the present paper we identify and study such an effect of unstable character observed experimentally in tunneling constant as a function of temperature for reactions with porphyrin. Also, we predict a stable cleavage in the temperature dependence of current in the artificial two-dimensional system, a pair of weakly coupled charged quantum dots with single electrons tunneling to superlattice substrate, and the associated fluctuations of quantum origin. We study the emerging effect of chaotization near the critical point of unstable cleavage for porphyrin.

In this paper, we continue to study bifurcation effects in two dimensional tunneling. In particular, we consider two-proton correlations of different types within the framework of dissipative quantum tunneling (instanton) approach. Moreover, we discuss a fine structure of bifurcations for systems with various potential energy surfaces [27, 28, 29, 30, 33, 34].

The layout of the paper is as follows.

In Section II, we introduce two-dimensional model potential energy surfaces for a pair of interacting particles. In Section III we present experimental aspects of the model. In Section IV, we study the effect of temperature on the tunneling rate. In Sections V and VI, we calculate the rate for the parallel and antiparallel tunneling and provide the analysis of the origin of bifurcation. The effect of a promoting mode (an environment) is studied in Section VII.

II. TWO-DIMENSIONAL POTENTIAL ENERGY SURFACES

Consider two charges that tunnel in two independent double-well potentials $U(q_1)$ and $U(q_2)$ presented as follows [7, 27, 28, 29]:

$$\begin{aligned} \tilde{U}(q_i) &= \frac{1}{2}\omega^2(q_i + a)^2\theta(-q_i) \\ &+ \left[-\Delta I + \frac{1}{2}\omega^2(q_i - b)^2 \right] \theta(q_i), \quad i = 1, 2, \end{aligned} \quad (1)$$

where the sum $a + b$ determines the length of a "link" in the corresponding macrocluster fragment; $\Delta I = \omega^2(b^2 - a^2)/2$ is a bias (an asymmetry parameter of the potential); $\theta(q_i)$ is a step function, and ω is the frequency (see discussion in Ref. [27]). The mass is absorbed into the definition of q .

The interaction between two charges, e.g., protons, is considered in a dipole-dipole approximation [28]

$$V_{\text{int}}(q_1, q_2) = -\frac{\alpha}{2}(q_1 - q_2)^2, \quad (2)$$

where α is a positive constant. We use the same interaction potential as in Ref. [6].

Thus, the total two-dimensional potential energy surface for parallel tunneling normalized by ω^2 , is given by

$$\begin{aligned} U_p(q_1, q_2) &= \frac{2\tilde{U}_p(q_1, q_2)}{\omega^2} = (q_1 + a)^2\theta(-q_1) \\ &+ [-(b^2 - a^2) + (q_1 - b)^2] \theta(q_1) + (q_2 + a)^2\theta(-q_2) \\ &+ [-(b^2 - a^2) + (q_2 - b)^2] \theta(q_2) - \frac{\alpha^*}{2}(q_1 - q_2)^2. \end{aligned} \quad (3)$$

Here, $\alpha^* = 2\alpha/\omega^2$ is the dimensionless parameter, $\alpha^* < 1$, $\alpha \simeq e^2/(\varepsilon R_0^3)$, e is the electron charge, R_0 is the separation distance between the reaction coordinates q_1 and q_2 of the tunneling particles; ε is the dielectric constant. The form of potential energy surface (3) is shown in Fig. 1.

For antiparallel transfer, the two-dimensional potential energy with the interaction term can be defined as

$$\begin{aligned} U_a(q_1, q_2) &= \frac{2\tilde{U}_a(q_1, q_2)}{\omega^2} = (q_1 + a)^2\theta(-q_1) \\ &+ [-(b^2 - a^2) + (q_1 - b)^2] \theta(q_1) + (q_2 - a)^2\theta(q_2) \\ &+ [-(b^2 - a^2) + (q_2 + b)^2] \theta(-q_2) - \frac{\tilde{\alpha}^*}{2}(q_1 - q_2)^2, \end{aligned} \quad (4)$$

where $\tilde{\alpha}^* = 2\tilde{\alpha}/\omega^2$ is a dimensionless parameter, $\tilde{\alpha}^* < 1$. The potential (4) is depicted in Fig. 2. The main difference between the potential energy surfaces (3) and (4) is in the initial location of the second particle, $\pm a$.

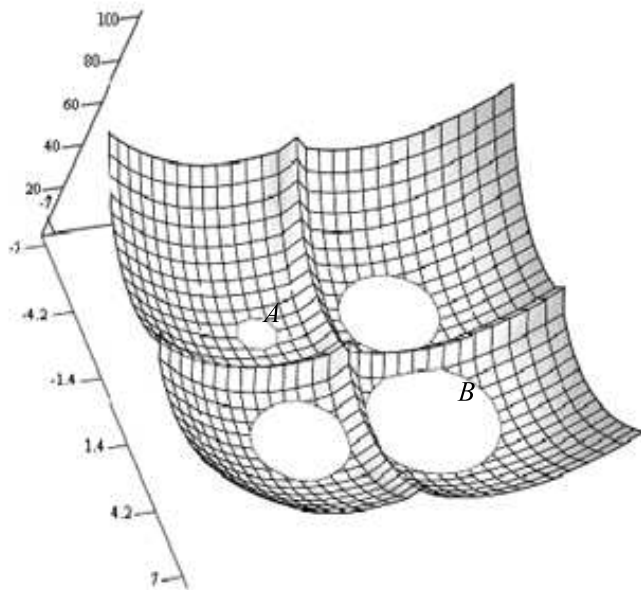


FIG. 1: Asymmetric potential energy surface (3) for parallel tunneling; $a = 2$, $b = 2.5$, $\alpha^* = 0.0001$. A and B indicate the initial and final states of the particles, respectively. The minimum of the potential at B is lower than that of at A . The other two (intermediate) minima are lower than those of at A and higher than at B .

The potential energy (3) can be referred to as "parallel" while the potential energy (4) as "antiparallel". We also define a "symmetric" potential energy as a particular case of the potential (4) under the condition $a = b$, i.e.,

$$U_s(q_1, q_2) = \frac{2\tilde{U}_s(q_1, q_2)}{\omega^2} = (q_1 + a)^2\theta(-q_1) + (q_1 - a)^2\theta(q_1) + (q_2 - a)^2\theta(q_2) + (q_2 + a)^2\theta(-q_2) - \frac{\tilde{\alpha}^{**}}{2}(q_1 - q_2)^2, \quad (5)$$

where the constant $\tilde{\alpha}^{**} < 1$. The potential energy (5) is presented in Fig. 3.

As shown in Refs. [28, 29, 33], such model potential energy surfaces well describe the dynamics in porphyrins (see also Sec. III below).

In many practical cases, the effect of a bath on particles' tunneling should be also included. In the next section we consider two particles embedded into a harmonic medium and linearly interacting with the bath modes.

III. EXPERIMENTAL ASPECTS OF THE MODEL

As it was mentioned in Introduction, adiabatic tunnel dissipative transfer appears to be very important in various physical and chemical processes [2]-[30]. It is of much interest to consider two-particle tunnel dissipative transfer of coupled charges. For example, a two-proton transfer can be characterized by a simultaneous tunneling and the changing of electronic structure which forms and breaks chemical bonds [24, 25, 26, 30]. One can consider, e.g., transfer of two protons in the dimer of 7-azaindole [26]; see Fig. 4.

It is particularly interesting to consider two-dimensional tunnel dynamics of coupled protons in a symmetric case of porphyrin molecules. For this symmetric reaction an unstable interchanging of the regimes of tunneling (synchronous regime is replaced by asynchronous one as temperature decreases) was observed for the first time. The interchanging corresponds to the instability cleavage in the dependence of the rate constant on temperature. In some aspect this picture resembles the effect predicted for interacting Josephson junctions [6]. In Fig. 5 we schematically present the

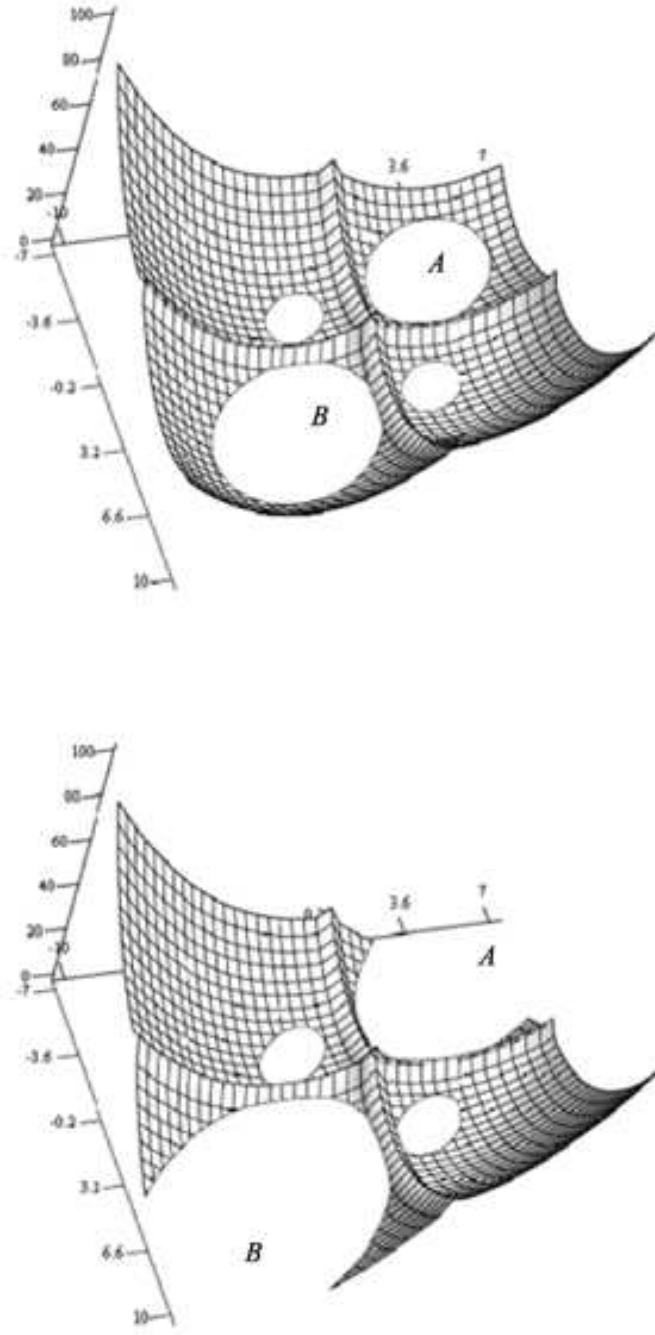


FIG. 2: Asymmetric potential energy surface (4) for antiparallel tunneling; (a) $a = 2$, $b = 2.3$, $\tilde{\alpha}^* = 0.1$ (top panel); (b) $a = 2$, $b = 2.3$, $\tilde{\alpha}^* = 0.5$ (bottom panel). A and B indicate initial and final states of the particles. The minimum of the potential at B is lower than that of at A . The other two (intermediate) minima are higher than those of at A and B .

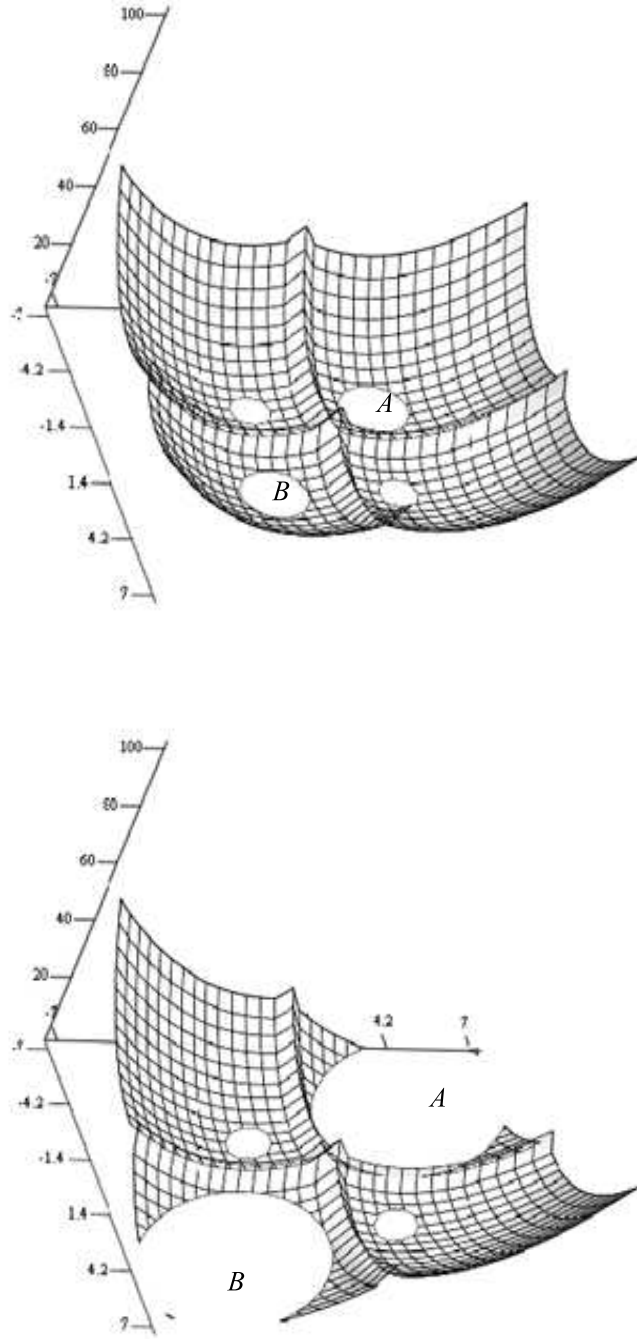


FIG. 3: Symmetric potential energy surface (5); (a) $a = 2$, $b = 2$, $\tilde{\alpha}^{**} = 0.1$ (top panel); (b) $a = 2$, $b = 2$, $\tilde{\alpha}^{**} = 0.5$ (bottom panel). A and B denote the initial and final states of the particles. The minimum of the potential energy at B is equal to that of at A . The other two (intermediate) minima are higher than those of at A and B .

FIG. 4: The dimer of 7-azaindole: (a) before the proton transfer, (b) after the proton transfer.

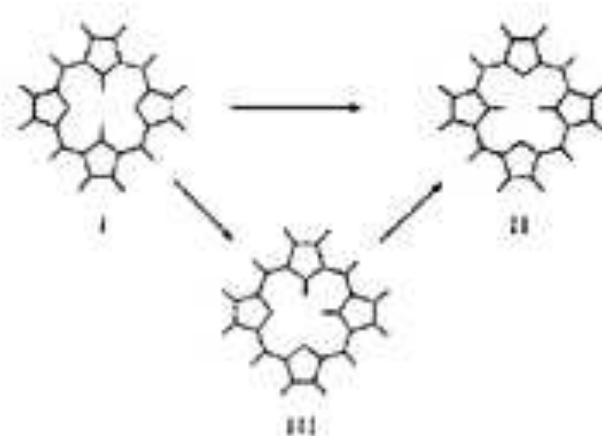


FIG. 5: A view of two equilibrium configurations, I and II, for the porphyrin molecule with the transfer of a pair of hydrogen atoms between nitrogen atoms. The intermediate (nonequilibrium) configuration III is characterized by the hydrogen atoms residing on the neighbor nitrogen atoms.

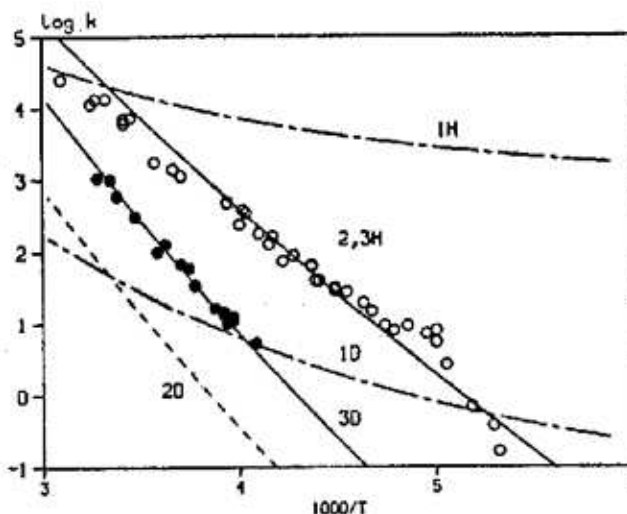


FIG. 6: Temperature dependence of the observed and predicted [24] rate constants in the reaction of the internal transfer of hydrogen (or deuterium) atoms in porphyrin molecule. Open and filled circles denote experimental data for the hydrogen and deuterium atoms respectively [35]. The lines denoted by 1H and 1D represent predicted curves [24] for a synchronous transfer of weakly coupled hydrogen and deuterium atoms respectively. The lines denoted 2H and 2D represent predicted curves for asynchronous transfer of weakly coupled hydrogen and deuterium atoms respectively. All the coupling constants J were scaled to reproduce the results for hydrogen atom transfer at $T = 300$ K. The used parameters are: the stretching and bending frequencies for the hydrogen atom are 3318 and 2482 cm^{-1} , for the deuterium atoms are 1223 and 1094 cm^{-1} respectively [36]; H and D stretching anharmonics and reduced masses are -80 and -50 cm^{-1} , and 1 and 2 respectively; the skeletal frequency is 380 cm^{-1} and the reduced mass is 2.8. The equilibrium separation N-H (N-D) is 400 pm. Endothermic value for an asynchronous mechanism is $\Delta E = -0.375$ eV, the coupling constant for synchronous transfer is $J = 0.016$ eV, the coupling constant for asynchronous transfer of weakly coupled atoms is $J = 0.23$ eV, the coupling constant for asynchronous transfer of strongly coupled atoms is $J = 0.70$ eV.

above mentioned reaction of the coupled protons transfer in porphyrin molecule. Fig. 6 [24] represents the experimental and the theoretically estimated temperature dependencies of the reaction rate for the transfer of internal hydrogen (or deuterium) atoms in porphyrin.

As it was mentioned by W. Siebrand (Div. of Chemistry, Nat. Research Council of Canada, Ottawa), a modified and extended microscopic model could be used to describe transfer charge transfer states in molecular dimers or crystals. Such states can be represented in the form $A^+A^- \leftrightarrow A^-A^+$ that formally corresponds to a two-electron transfer. Two types of dimers corresponding to $+$ and $-$ combinations are separated by the band which is associated to the frequency of the transfer. None of these states have a constant dipole moment but an external field can mix them and induce a quite considerable dipole moment.

In experiments, the dependence of the absorption spectrum of such systems on the external field was measured. The results were interpreted in terms of charge-transfer excitons. This interpretation is valid only if the external field is sufficiently strong, namely, to be able to break the symmetry.

Therefore, it is of much interest to investigate splitting in the spectrum of charge-transfer dimer. In early studies one neglected an electron-electron interaction that appears to be of much importance here. The splitting seems to be much smaller than it was estimated earlier. In terms of the model presented below, electrons are attracted by Coulomb force of positive molecular ions and repel each other. Since the instantaneous situation when the electrons are at equal distance from the two molecules is energetically not favorable, a high barrier for the transfer is formed. An asynchronous transfer gives an intermediate state corresponding to highly excited vibronic state so that this type of transfer is not favorable due to Frank-Condon factors.

Also, this state rapidly undergoes vibronic relaxation that corresponds to a non-radiative decay of charge-transfer states [37]. As the result, it is still important to describe the observed properties in terms of controlled processes of electron transfer. Although W. Siebrand expressed some doubts on the possibility of a direct use of the model presented below to the two-proton transfer in porphyrin-type systems, he pointed out that there is a possibility to use such a nonlinear two-particle model in studying experimentally observed effectively two-dimensional (and two-particle) electron transfer.

The microscopic model suggested in this paper allows one to interpret the experimental data, and provides complete

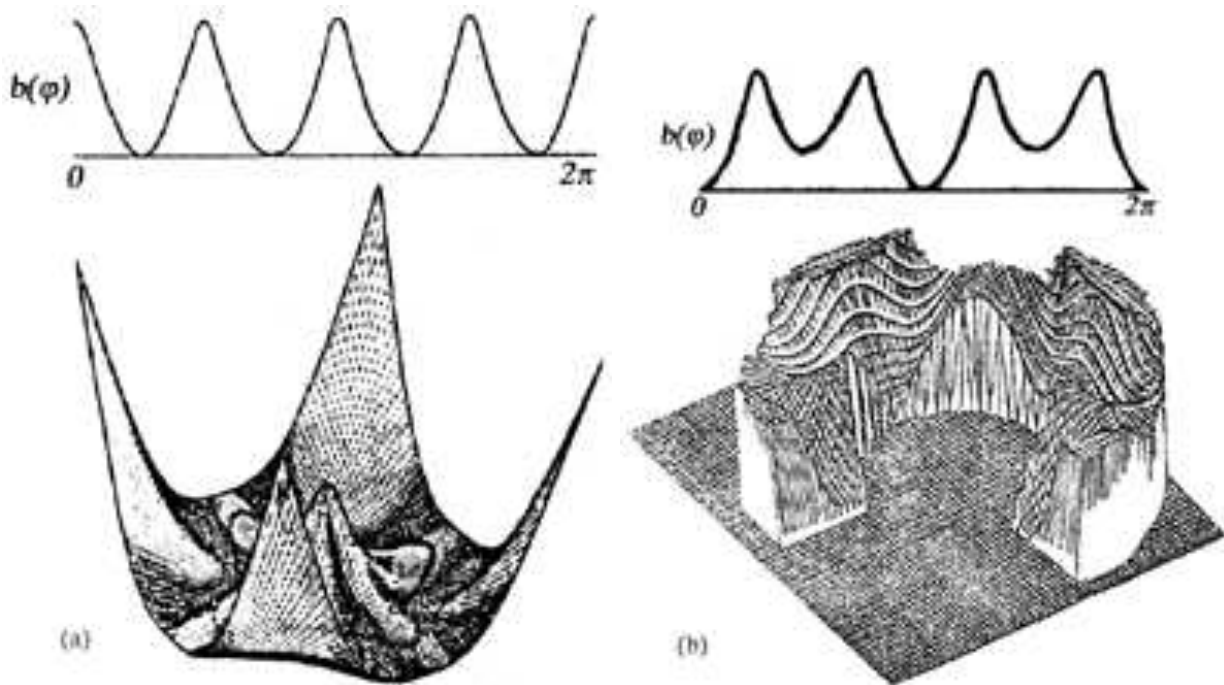


FIG. 7: Two-dimensional adiabatic potential and the path characterized by a minimal energy for (a) synchronous and (b) asynchronous mechanisms of NH-tautometry.

qualitative and good quantitative description. Also, the model allows one to determine the critical point in an analytically exact manner (in the quasiclassical approximation), both the temperature and the coupling coefficient, that is an interesting theoretical result which is analogous to that of Ref. [6]. As an indirect confirmation of applicability of the microscopic model we mention a comparison with the results of modelling of the potential energy surface in porphyrins [30].

For the case of 7-azaindole dimer, the protons are initially reside closely to nitrogen atoms in the corresponding 5-chain "rings" of the dimer. When two coupled molecules of 7-azaindole form a dimer there may occur a cooperative (tunnel) two-proton transfer. The protons are moved to nitrogen atoms of 6-chain "rings" of the dimer. The proton transfer is accompanied by changing of the structure of orbitals of electrons. A synchronous transfer of two protons appears to be energetically preferable while the independent tunneling of the protons becomes forbidden due to the changing of the structure of orbitals.

In Sections below, we consider a synchronous tunnel transfer of two weakly coupled particles. For two uncoupled particles, each of the particles moves independently in the proper double-well potential. We will study the effect of coupling to oscillators (an environment) at independent (*asynchronous*) and cooperative (*synchronous*) tunneling of the particles. Also, we will investigate fine structure of the arising two-dimensional bifurcations which occur during the changing of regimes.

As it was mentioned above, the study of temperature-dependent NMR spectra of porphyrins (compounds of this class are known to play an important role in biological processes) revealed intermolecular regrouping (see Fig. 5). To describe this regrouping two mechanisms are suggested: (i) the *synchronous* one (which is associated to a synchronous transfer of two NH hydrogens) and (ii) the *asynchronous* one (with consecutive transfer of one of the particles).

Two-dimensional potential energy surfaces (PES) $V(r, \varphi)$ have been calculated by using INDO and we represent them in the following analytical way:

$$V(r, \varphi) = C[a(\varphi)(r - r_{\min}(\varphi))^2 + b(\varphi)]. \quad (6)$$

The synchronous case:

$$\begin{aligned} b(\varphi) = & 1.355 + 1.681 \cos(4\varphi) + 0.488 \cos(8\varphi) \\ & + 0.289 \cos(12\varphi) + 0.147 \cos(16\varphi) + 0.049 \cos(20\varphi) \\ & + 0.023 \cos(24\varphi) \text{ eV}, \end{aligned} \quad (7)$$

$$r_{min}(\varphi) = 1.00 - 0.14 \cos(4\varphi) \text{ \AA}, \quad (8)$$

$$a(\varphi) = 38.1 \cos(4\varphi) + 50.8 \text{ eV/\AA}^2. \quad (9)$$

The asynchronous case:

$$b(\varphi) = 0.829 - 0.183 \cos(2\varphi) + 0.821 \cos(4\varphi) + 0.260 \cos(8\varphi) - 0.077 \cos(12\varphi) \text{ eV}, \quad (10)$$

$$r_{min}(\varphi) = 1.00 - 0.14 \cos(4\varphi) \text{ \AA}, \quad (11)$$

$$a(\varphi) = 19.05 \cos(4\varphi) + 25.4 \text{ eV/\AA}^2. \quad (12)$$

The potential along the path characterized by a minimal energy and PES $V(r, \varphi)$ are illustrated in Fig. 7.

By comparing of the chosen model potential (see Fig. 3) with that of Fig. 7 one can see that the chosen model potential corresponds to a realistic PES for porphyrin. More details on PES for porphyrin have been discussed in Ref. [30].

IV. TWO-PARTICLE TRANSITION PROBABILITY

We assume that two particles independently interact with a harmonic bath. Such interaction is considered in a bilinear approximation. The dynamics of the environment is described by the oscillator Hamiltonian (we use $\hbar = 1$, $k_B = 1$ units with the oscillators' masses equal to one),

$$H_{ph} = \frac{1}{2} \sum_i (P_i^2 + \omega_i^2 Q_i^2). \quad (13)$$

Each of the tunneling particles (electrons or effective charges) interacts with the oscillator bath in the following way:

$$V_{p-ph}^{(1)}(q_1, Q_i) = q_1 \sum_i C_i Q_i, \quad V_{p-ph}^{(2)}(q_2, Q_i) = q_2 \sum_i C_i Q_i, \quad (14)$$

As in Ref. [28], we are interested in the transition probability per unit time or, more precisely, only in its exponential part which can be written in the Langer's form,

$$\Gamma = 2T \frac{\text{Im}Z}{\text{Re}Z}. \quad (15)$$

In such a consideration, metastable levels can be presented as

$$\Gamma = -2 \text{Im}E, \quad E = E_0 - i\Gamma/2. \quad (16)$$

It should be emphasized that Eq. (15) is valid only for temperatures below the crossover temperature while for higher temperatures a different prefactor is required [23].

Equation (15) is obtained by generalizing the expression (16) to nonzero temperatures [2, 3, 4, 5, 6, 7, 8, 9, 10, 11, 12, 13, 14, 15, 16, 17]

$$\Gamma = \frac{2 \sum e^{-E_{0i}/T} \text{Im}E_i}{e^{-E_{0i}/T}} = \frac{2T \text{Im} \sum e^{-E_i/T}}{\text{Re} \sum e^{-E_i/T}} = \frac{2T \text{Im}Z}{\text{Re}Z}. \quad (17)$$

Here, i labels the energy levels in the metastable state, Z is the partition function of the system, and T is the temperature.

To calculate Γ , it is convenient to present Z in the form of a path integral [2, 3, 4, 5, 6, 7, 8, 9, 10, 11, 12, 13, 14, 15, 16, 17]

$$Z = \prod_i \int Dq_1 Dq_2 DQ_i \exp[-S\{q_1, q_2, Q_i\}]. \quad (18)$$

Here, S denotes an underbarrier action for the total system. The imaginary part $\text{Im}Z$ is due to the decay of the energy states in the initial well. The validity of this approximation requires dissipation to be strong enough so that only an incoherent decay occurs [23]. The imaginary part in the partition function with a double well potential energy can be also explained due to the strong dissipation to the bath. Indeed, the particles do not come back to their initial state. Coherent oscillations can happen only if the interaction with bosons is weak enough [8] or the bath is in nonequilibrium state [38, 40].

The integral (18) can be performed over phonon coordinates [28] resulting in

$$S\{q_1, q_2\} = \int_{-\beta/2}^{\beta/2} d\tau \left[\frac{1}{2} \dot{q}_1^2 + \frac{1}{2} \dot{q}_2^2 + V(q_1, q_2) \right. \\ \left. + \int_{-\beta/2}^{\beta/2} d\tau' D(\tau - \tau') [q_1(\tau) + q_2(\tau)] [q_1(\tau') + q_2(\tau')] \right], \quad (19)$$

where

$$D(\tau) = \frac{1}{\beta} \sum_{n=-\infty}^{\infty} D(\nu_n) e^{i\nu_n \tau}, \quad (20)$$

$\beta = \hbar/(k_B T)$ is an inverse temperature (below we assume that $\hbar = 1$ and $k_B = 1$), $\nu_n = 2\pi n/\beta$ is the Matsubara's frequency, and

$$D(\nu_n) = - \sum_i \frac{C_i^2}{\omega_i^2 + \nu_n^2}. \quad (21)$$

A trajectory that minimizes the Euclidean action S can be found from the equations of motion. In particular, we embark on the antiparallel tunneling

$$- \ddot{q}_1 + \Omega_0^2 q_1 + \tilde{\alpha}_1 q_2 + \int_{-\beta/2}^{\beta/2} d\tau' K(\tau - \tau') [q_1(\tau') + q_2(\tau')] \\ + \omega^2 a \theta(-q_1) - \omega^2 b \theta(q_1) = 0, \quad (22)$$

$$- \ddot{q}_2 + \Omega_0^2 q_2 + \tilde{\alpha}_1 q_2 + \int_{-\beta/2}^{\beta/2} d\tau' K(\tau - \tau') [q_1(\tau') + q_2(\tau')] \\ - \omega^2 a \theta(q_2) + \omega^2 b \theta(-q_2) = 0. \quad (23)$$

In Eqs. (22) and (23) the kernel K is defined by

$$K(\tau) = \frac{1}{\beta} \sum_{n=-\infty}^{\infty} \xi_n e^{i\nu_n \tau}. \quad (24)$$

Here, ξ_n is the Green's function defined by Eq. (21) without the zero-frequency term,

$$D(\nu_n) = - \sum_i \frac{C_i^2}{\omega_i^2} + \xi_n. \quad (25)$$

Thus, we seek for solutions of Eqs. (22) and (23) by expanding the trajectories $q_1(t)$ and $q_2(t)$ into Fourier series,

$$q_1 = \frac{1}{\beta} \sum_{n=-\infty}^{\infty} q_n^{(1)} e^{i\nu_n \tau}, \quad q_2 = \frac{1}{\beta} \sum_{n=-\infty}^{\infty} q_n^{(2)} e^{i\nu_n \tau}. \quad (26)$$

Introducing the renormalized frequency and interaction constant,

$$\Omega_0^2 = \omega^2 - \sum_i \frac{C_i^2}{\omega_i^2} - \tilde{\alpha}, \quad \tilde{\alpha}_1 = \tilde{\alpha} - \sum_i \frac{C_i^2}{\omega_i^2}, \quad (27)$$

respectively, and substituting Eqs. (26) into Eqs. (22) and (23), we obtain that for $n = 0$,

$$\begin{aligned} q_0^{(1)} + q_0^{(2)} &= \frac{2\omega^2(a+b)\varepsilon}{\Omega_0^2 + \tilde{\alpha}_1}, \\ q_0^{(1)} - q_0^{(2)} &= -\frac{2\omega^2 a \beta}{\Omega_0^2 - \tilde{\alpha}_1} + \frac{4\omega^2(a+b)\tau_0}{\Omega_0^2 - \tilde{\alpha}_1}, \end{aligned} \quad (28)$$

and for $n \neq 0$,

$$\begin{aligned} q_n^{(1)} + q_n^{(2)} &= \frac{2\omega^2(a+b)(\sin \nu_n \tau_1 - \sin \nu_n \tau_2)}{\nu_n(\nu_n^2 + \Omega_0^2 + \tilde{\alpha}_1 + 2\xi_n)}, \\ q_n^{(1)} - q_n^{(2)} &= \frac{2\omega^2(a+b)(\sin \nu_n \tau_1 + \sin \nu_n \tau_2)}{\nu_n(\nu_n^2 + \Omega_0^2 - \tilde{\alpha}_1)}. \end{aligned} \quad (29)$$

Here, we have introduced the following notation:

$$\varepsilon = \tau_1 - \tau_2, \quad \tau_0 = (\tau_1 + \tau_2)/2. \quad (30)$$

The time instants τ_1 and τ_2 , at which the particles pass the top points of the barrier, are determined from the following equations:

$$q_1(\tau_1) = 0, \quad q_2(\tau_2) = 0. \quad (31)$$

Equations (31) allow us to change the argument of the θ -function. Namely, instead of the q_1 - and q_2 -dependencies, we can use a time-dependent θ -function. This reduces Eqs. (22) and (23) to a linear form.

Finally, substituting the trajectory determined from Eqs. (26), (28) and (29) into Eq. (19), we arrive at the following expression for the instanton action:

$$\begin{aligned} S &= \frac{4\omega^4 a(a+b)\tau_0}{\Omega_0^2 - \tilde{\alpha}_1} - \frac{\omega^4(a+b)^2\varepsilon^2}{\beta(\Omega_0^2 + \tilde{\alpha}_1)} - \frac{4\omega^4(a+b)^2\tau_0^2}{\beta(\Omega_0^2 - \tilde{\alpha}_1)} \\ &\quad - \frac{8\omega^4(a+b)^2}{\beta} \sum_{n=1}^{\infty} \left[\frac{\sin^2 \nu_n \tau_0 \cdot \cos^2(\nu_n \varepsilon/2)}{(\nu_n^2 + \Omega_0^2 - \tilde{\alpha}_1)\nu_n^2} \right. \\ &\quad \left. + \frac{\cos^2 \nu_n \tau_0 \cdot \sin^2(\nu_n \varepsilon/2)}{(\nu_n^2 + \Omega_0^2 + \tilde{\alpha}_1 + 2\xi_n)\nu_n^2} \right]. \end{aligned} \quad (32)$$

V. PARALLEL PARTICLE TUNNELING

For the case of parallel particle tunneling, the Euclidean action S can be determined similarly to antiparallel tunneling [see Eqs. (22) and (23)]. The trajectory minimizing the Euclidean action (instanton), can be determined from the equations of motion. As in the previous section, we seek for solutions of these equations in the form of the Fourier expansion (26). The time instants τ_1 and τ_2 are determined by Eqs. (31).

In the case of parallel tunneling particles [the potential energy (3)], the resulting Euclidean action is given as follows:

$$\begin{aligned} S &= 2a(a+b)(\tau_1 + \tau_2)\omega^2 - \frac{1}{\beta}\omega^2(a+b)^2(\tau_1 + \tau_2)^2 \\ &\quad - \frac{\omega^4(a+b)^2(\tau_1 - \tau_2)^2}{(\omega^2 - 2\alpha)\beta} \\ &\quad - \frac{2\omega^4(a+b)^2}{\beta} \sum_{n=1}^{\infty} \left[\frac{(\sin \nu_n \tau_1 + \sin \nu_n \tau_2)^2}{\nu_n^2(\nu_n^2 + \omega^2 + \xi_n)} \right. \\ &\quad \left. + \frac{(\sin \nu_n \tau_1 - \sin \nu_n \tau_2)^2}{\nu_n^2(\nu_n^2 + \omega^2 - 2\alpha)} \right], \end{aligned} \quad (33)$$

where ξ_n is defined by Eq. (25).

Below, we use the following notation:

$$\varepsilon = \varepsilon^* \omega = (\tau_1 - \tau_2) \omega,$$

$$\tau = 2\tau^* \omega = (\tau_1 + \tau_2) \omega,$$

$$\beta^* = \beta \omega / 2,$$

$$\alpha^* = 2\alpha / \omega^2,$$

$$b^* = b/a,$$

and assume that

$$b \geq a.$$

In the absence of interaction with an oscillator bath, i.e., at $\xi_n = 0$, the action (33) as a function of the parameters ε and τ yields

$$\begin{aligned} S = & \frac{(a+b)^2 \omega}{2} \left\{ \frac{4a\tau}{a+b} - \frac{\tau}{a+b} \left(1 + \frac{1}{1-\alpha^*} \right) \right. \\ & + \frac{(\tau-|\varepsilon|)\alpha^*}{1-\alpha^*} + \coth \beta^* - \sinh^{-1} \beta^* [\cosh(\beta^* - \tau) \cosh \varepsilon \\ & \quad + \cosh(\beta^* - \tau) - \cosh(\beta^* - |\varepsilon|)] \\ & \quad - (1-\alpha^*)^{-3/2} [-\coth(\beta \sqrt{1-\alpha^*}) \\ & \quad + \sinh^{-1}(\beta \sqrt{1-\alpha^*}) [\cosh((\beta^* - \tau) \sqrt{1-\alpha^*}) \\ & \quad \times (\cosh(\varepsilon \sqrt{1-\alpha^*}) - 1) + \cosh((\beta^* - |\varepsilon|) \sqrt{1-\alpha^*})]] \left. \right\}. \end{aligned} \quad (34)$$

As soon as the trajectory is found, Eqs. (31) can be presented in the following form:

$$\begin{aligned} & \sinh \varepsilon [\cosh \tau \coth \beta^* - \sinh \tau - \coth \beta^*] + \\ & \frac{1}{1-\alpha^*} \sinh(\varepsilon \sqrt{1-\alpha^*}) [\cosh(\tau \sqrt{1-\alpha^*}) \coth(\beta^* \sqrt{1-\alpha^*}) \\ & \quad - \sinh(\tau \sqrt{1-\alpha^*}) + \coth(\beta^* \sqrt{1-\alpha^*})] = 0, \\ & 3 - \frac{4}{1+b^*} - \frac{1}{1-\alpha^*} + \cosh \varepsilon [\sinh \tau \coth \beta^* - \cosh \tau \\ & \quad - 1] + \sinh \tau \coth \beta^* - \cosh \tau \\ & \quad + \frac{1}{1-\alpha^*} \cosh(\varepsilon \sqrt{1-\alpha^*}) [\sinh(\tau \sqrt{1-\alpha^*}) \\ & \quad \times \coth(\beta^* \sqrt{1-\alpha^*}) - \cosh(\tau \sqrt{1-\alpha^*}) + 1] \\ & \quad - \frac{1}{1-\alpha^*} [\sinh(\tau \sqrt{1-\alpha^*}) \coth(\beta^* \sqrt{1-\alpha^*}) \\ & \quad - \cosh(\tau \sqrt{1-\alpha^*})] = 0. \end{aligned} \quad (35)$$

Simple analytic solutions of Eqs. (35) are obtained in the particular case when

$$\begin{aligned} \varepsilon &= (\tau_1 - \tau_2) \omega = 0, \quad \forall \beta, \alpha < \omega^2/2, \\ \tau_1 = \tau_2 &= \frac{\tau}{2\omega} = \frac{1}{2\omega} \operatorname{arcosh} \left[\frac{1-b^*}{1+b^*} \sinh \frac{\beta \omega}{2} \right] + \frac{\beta}{4}. \end{aligned} \quad (36)$$

However, a complete analysis requires numerical studies.

At sufficiently low temperatures, $\omega\beta \gg 1$, for $1 < b/a < 3$, and

$$\frac{b-a}{2(b+a)} \leq \frac{2\alpha}{\omega^2} < \alpha_c^* \equiv \frac{2(b-a)}{3b-a},$$

we finally obtain, with the exponential accuracy,

$$\begin{aligned} e^{-\tau\sqrt{1-\alpha^*}} &\simeq \left[3 - \frac{4}{1+b^*} - \frac{1}{1-\alpha^*}\right](1-\alpha^*)^{1/(1-\sqrt{1-\alpha^*})} \\ &\times \left\{1 + (1-\alpha^*)^{1/(1-\sqrt{1-\alpha^*})} \left[-\frac{1}{1-\alpha^*} + \left(3 - \frac{4}{1+b^*} - \frac{1}{1-\alpha^*}\right)/(1-\sqrt{1-\alpha^*})\right]\right\}^{-1}, \\ e^{-\varepsilon} &\simeq \left[3 - \frac{4}{1+b^*} - \frac{1}{1-\alpha^*}\right]e^{\tau\sqrt{1-\alpha^*}} + \frac{1}{1-\alpha^*}. \end{aligned} \quad (37)$$

The solution (37) is valid at

$$\beta > \beta_c \equiv \frac{\tau\sqrt{1-\alpha^*}}{\omega}. \quad (38)$$

We point out that an approximate solution can be found for large values of the parameter b^* (and small α^*). However, below we focus on the more important solution (37). The analysis indicates that there are no perturbative solutions of Eqs. (35) at low temperatures and small ε .

For $\varepsilon = 0$ [see Eq. (36)], the action (34) results in

$$\begin{aligned} S_{\varepsilon=0} &= \omega(b^2 - a^2) \operatorname{arcosh} \left[\frac{b^* - 1}{b^* + 1} \sinh \frac{\omega\beta}{2} \right] \\ &\quad - \frac{1}{2} \omega^2 (b^2 - a^2) \beta + \omega(b+a)^2 \left[\cosh \frac{\omega\beta}{2} \right. \\ &\quad \left. - \left(1 + \frac{(b^* - 1)^2}{(b^* + 1)^2} \sinh^2 \frac{\omega\beta}{2} \right)^{1/2} \right] \sinh^{-1} \frac{\omega\beta}{2}. \end{aligned} \quad (39)$$

The action (39) coincides (up to a factor of two) with that of calculated in Ref. [27]. Thus, we have calculated the two-particle Euclidean action for the case of synchronous parallel motion of the two interacting particles.

In the symmetric case ($b^* = 1$), the action (39) reduces to

$$S_{\varepsilon=0}^{a=b} = 4\omega^2 \tanh \frac{\omega\beta}{4}. \quad (40)$$

At $b^* > 1$, the character of the temperature dependence is almost the same.

At $\varepsilon \neq 0$, the corresponding action S can be obtained by substituting Eq. (37) into Eq. (34) (for brevity, this cumbersome expression is omitted). A simple analysis shows that $S_{\varepsilon \neq 0} < S_{\varepsilon=0}$. Moreover, it appears that the difference $\Delta S = S_{\varepsilon \neq 0} - S_{\varepsilon=0}$ has a maximum at $\omega\beta \gg 1$.

The tunneling paths (26) are presented by the solutions (36) and (37). At the critical point, $\beta = \beta_c$, defined by Eq. (38), a relatively abrupt change in the dynamics results in a splitting of the single trajectory ($\varepsilon = 0$) into two ($\varepsilon \neq 0$), as shown in Fig. 8.

At $\beta > \beta_c$, i.e., for temperatures below the critical temperature, $T < T_c$, only a split trajectory ($\varepsilon \neq 0$) occurs since $S_{\varepsilon \neq 0} < S_{\varepsilon=0}$ (see Fig. 9).

When $\beta < \beta_c$, i.e., at $T > T_c$, and $\alpha > \alpha_c$ [see Eq. (37)], the solution is determined by a single trajectory. We have also found that the single trajectory solution holds in the whole temperature range for a symmetric potential energy ($b^* = 1$).

The above consideration is based on the analytic solutions (36) for $\tau_{1,2}$ near the critical point. A complete analysis of Eq. (35) requires more detail.

The numerical study of the set of transcendental equations (35) reveals remarkable features of two-dimensional tunneling. The value of the critical parameter α_c decreases with temperature as shown in Figs. 10, 11, and 12. The temperature dependence of α_c indicates to the existence of a finite low-temperature limit. It becomes clear that the weaker the interaction between the tunneling particle, the lower temperatures are required for the synchronous

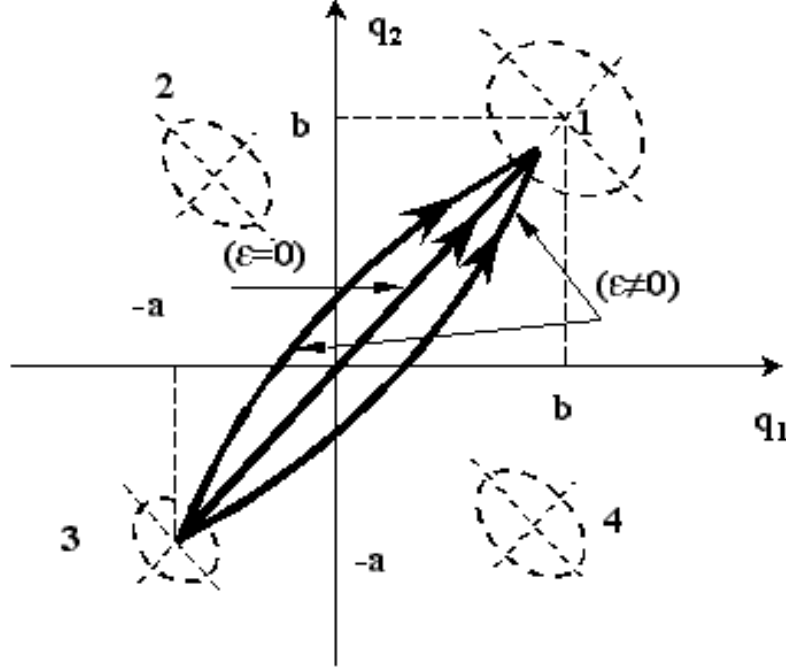


FIG. 8: Trajectories (a single path is characterized by $\varepsilon = 0$ and a splitted path is characterized by $\varepsilon \neq 0$) for two parallel moving particles, at $\omega\beta \gg 1$; (1)-(4) label the projections of the minima of potential energy (3).

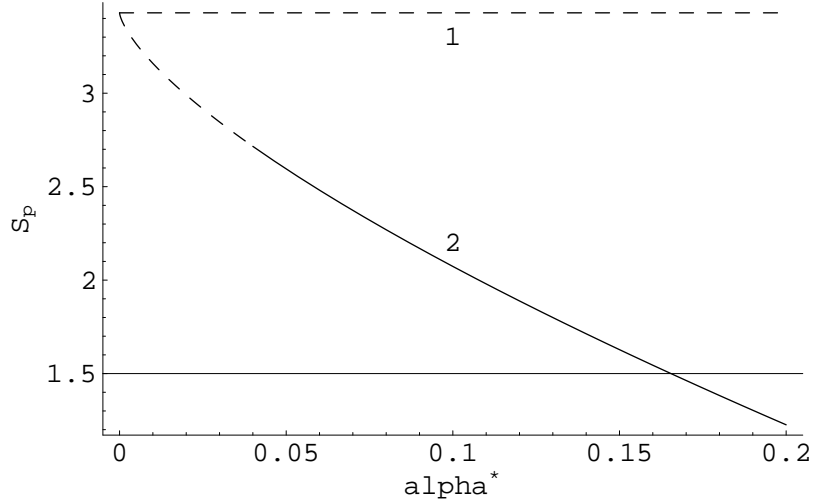


FIG. 9: Instanton action as a function of the interaction parameter $\alpha^* = 2\alpha/\omega^2$ of the two parallel moving particles, at $\omega\beta \gg 1$; $S_p = S/(\omega a^2)$; (1) is the single trajectory; (2) is the split trajectory.

tunneling. Since the synchronous tunneling is valid only for $T < T_c$ [see Eq. (38)] the dependence of β_c on the interaction parameter reveals that the minimum occurs at $\alpha^* = 0.2$. The nonmonotonic behavior of β_c as a function of α^* can be explained by the α^* -dependence of τ as well.

Additionally, the curve in Fig. 12 exhibits an anomalous behavior (an increasing part of the curve) that can be explained in the following way: a two-dimensional potential energy for parallel tunneling is evidently deformed by an increase of the interaction constant. Indeed, the minima of the potential surface become lower and the distance between them is larger. Small deformations in the potential energy surface change the contribution produced by the

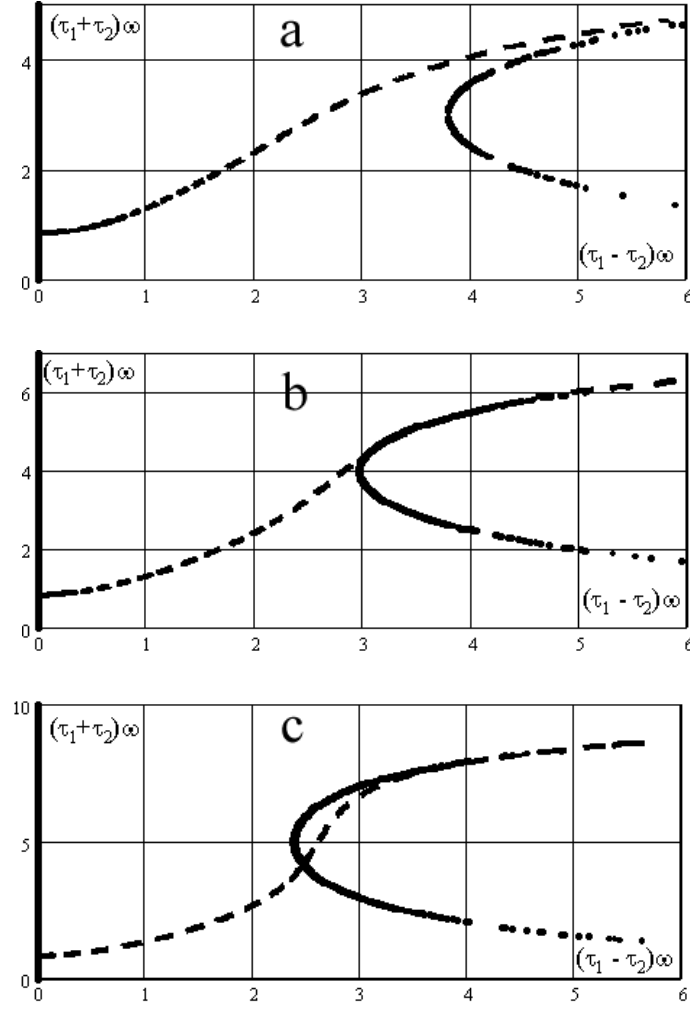


FIG. 10: Numerical solutions of transcendental equations (35). In addition to the studied solution $\tau_1 = \tau_2$, with larger β there are additional solutions, $\tau_1 \neq \tau_2$, shown in panels (b) and (c). Panel (b) reveals a *single* additional solution corresponding to the lower value of the Euclidean action. Panel (c) shows two different additional solutions with the one corresponding to the lower value of the action.

temperature increase towards a synchronous character of the tunneling. However, for sufficiently large deformations of the potential, the situation is a quite opposite. The significant deformations are in favor of synchronous transfer. Thus, an increase in the interaction constant provides a similar effect when temperature increases. Such a behavior takes place up to the certain value of the interaction constant, beyond which the potential energy surface becomes strongly perturbed. Thus, Figs. 11 and 12 are complimentary to each other. Consequently, Fig. 12 can be viewed as a bifurcation diagram. Indeed, the region below the curve corresponds to the synchronous tunneling, while the region above the curve corresponds to the asynchronous one.

Fig. 10 demonstrates how the critical parameter β_c changes from synchronous to asynchronous values with temperature. Figs. 10b and 10c reveal the existence of the additional points, referred to as the bifurcation points, corresponding to the change of tunneling regimes. For the two bifurcation points shown in Fig. 10c, only one is physical because it corresponds to the lower value of the action (the second point is metastable). However, for sufficiently small differences between the values of the action at these bifurcation points, *both* close points contribute, thus leading to corresponding "fluctuations" in the system during the change of the regimes. For lower temperatures, such fluctuations become negligible because two bifurcation points contributes differently. Thus, a stable character of the asynchronous tunnel transfer is achieved due to a much lower value of the action at one of the bifurcation points.

For chemical reactions mentioned in Introduction, the effect of the change in the tunneling regimes reveals as a *cleavage* in the experimental temperature dependence of the tunneling constant. Fine details of this instability have not been studied yet. Nevertheless, the very existence of instability at the edge of the bifurcation can be explained

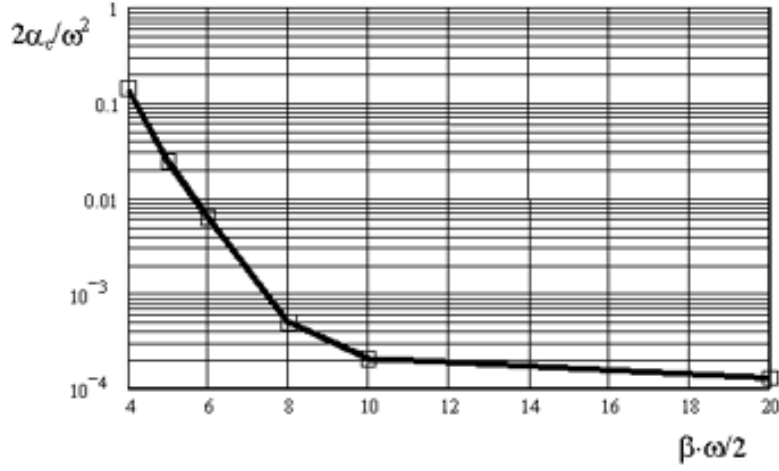


FIG. 11: Parameter α_c as a function of inverse temperature, at the fixed value of the frequency ω and asymmetry parameter b^* .

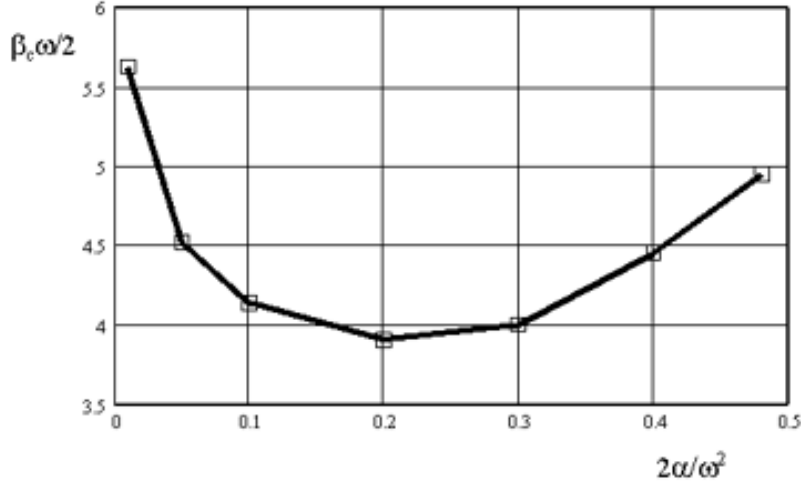


FIG. 12: Parameter β_c is presented as a function of the interaction parameter of the two tunneling particles.

as the result of specific fluctuations. A numerical analysis of the bifurcations in antiparallel tunneling is given in the next section.

VI. TWO-DIMENSIONAL ANTIPARALLEL TUNNELING

For antiparallel tunneling of two particles [see the potential energy (4)], the instanton action as a function of the parameters ε and τ is determined by Eq. (32). For $\xi_n = 0$, we obtain

$$\begin{aligned}
 S = & -\frac{\omega\tau(b^2 - a^2)}{1 - \tilde{\alpha}^*} - \frac{\omega(a + b)^2}{2} \left\{ |\varepsilon| \left(1 - \frac{1}{1 - \tilde{\alpha}^*} \right) \right. \\
 & + \frac{\sinh(|\varepsilon|\sqrt{1 - \tilde{\alpha}^*})}{(1 - \tilde{\alpha}^*)^{3/2}} - \sinh|\varepsilon| + \frac{\cosh(\varepsilon\sqrt{1 - \tilde{\alpha}^*}) + 1}{(1 - \tilde{\alpha}^*)^{3/2}} \\
 & \times [\sinh(\beta^*\sqrt{1 - \tilde{\alpha}^*})]^{-1} [\cosh((\beta^* - \tau)\sqrt{1 - \tilde{\alpha}^*}) \\
 & \quad \left. - \cosh(\beta^*\sqrt{1 - \tilde{\alpha}^*})] \right\}
 \end{aligned}$$

$$+\frac{\cosh\varepsilon-1}{\sinh\beta^*}[\cosh(\beta^*-\tau)+\cosh\beta^*]\Big\}.$$
 (41)

The parameters ε and τ are found from the following set of equations [see Eq. (31)]:

$$\begin{aligned} & -\sinh\varepsilon[\coth\beta^*+\cosh\tau\coth\beta^*-\sinh\tau] \\ & +\frac{1}{1-\tilde{\alpha}^*}\sinh(\varepsilon\sqrt{1-\tilde{\alpha}^*})[\coth(\beta^*\sqrt{1-\tilde{\alpha}^*}) \\ & -\cosh(\tau\sqrt{1-\tilde{\alpha}^*})\coth(\beta^*\sqrt{1-\tilde{\alpha}^*}) \\ & +\sinh(\tau\sqrt{1-\tilde{\alpha}^*})]=0, \\ & -1-\frac{4}{(1+b^*)(1-\tilde{\alpha}^*)}+\frac{1}{1-\tilde{\alpha}^*} \\ & +(\cosh\varepsilon-1)(\sinh\tau\coth\beta^*-\cosh\tau) \\ & +\cosh\varepsilon+\frac{1}{1-\tilde{\alpha}^*}\left\{[\cosh(\varepsilon\sqrt{1-\tilde{\alpha}^*})+1] \right. \\ & \times[\sinh(\tau\sqrt{1-\tilde{\alpha}^*})\coth(\beta^*\sqrt{1-\tilde{\alpha}^*}) \\ & \left. -\cosh(\tau\sqrt{1-\tilde{\alpha}^*})]-\cosh(\varepsilon\sqrt{1-\tilde{\alpha}^*})\right\}=0. \end{aligned}$$
 (42)

Simple analytic solutions of Eqs. (42) can be obtained in the following form:

$$\begin{aligned} \varepsilon &= (\tau_1 - \tau_2)\omega = 0, \quad \forall \beta, \quad \tilde{\alpha} < \omega^2/2, \\ \tau_1 &= \tau_2 = \frac{\tau}{2\omega} \\ &= \frac{1}{2\omega\sqrt{1-\tilde{\alpha}^*}} \operatorname{arcosh} \left[\frac{1-b^*}{1+b^*} \sinh\left(\frac{\beta\omega}{2}\sqrt{1-\tilde{\alpha}^*}\right) \right] + \frac{\beta}{4}. \end{aligned}$$
 (43)

Similarly to the case of parallel tunneling, we obtain that at low temperatures, $\omega\beta \gg 1$, with the exponential accuracy,

$$\begin{aligned} e^{-\tau\sqrt{1-\tilde{\alpha}^*}} &\simeq \frac{A(1-\tilde{\alpha}^*)^{1/\gamma}}{1-(1-\tilde{\alpha}^*)^{1/\gamma}(A/\gamma-(1-\tilde{\alpha}^*)^{-1})}, \\ e^\varepsilon &\simeq Ae^{\tau\sqrt{1-\tilde{\alpha}^*}} - \frac{1}{1-\tilde{\alpha}^*}. \end{aligned}$$
 (44)

Here,

$$A = -1 - \frac{4}{(1+b^*)(1-\tilde{\alpha}^*)} + \frac{3}{1-\tilde{\alpha}^*}, \quad \gamma = 1 - \sqrt{1-\tilde{\alpha}^*},$$

while $\tilde{\alpha}^*$, b^* , ε , and τ are determined as for the parallel transfer.

The solution (44) is valid at $\tilde{\alpha}_{c1}^* < \tilde{\alpha}^* < \tilde{\alpha}_{c2}^*$, where the lower and upper bounds $\tilde{\alpha}_{c1}^*$ and $\tilde{\alpha}_{c2}^*$ are derived from a cumbersome transcendental equation (for brevity it is not presented here). Particularly, in the symmetric case, $b^* = 1$, we obtain the condition in a simple analytic form, $1/4 < 2\tilde{\alpha}/\omega^2 < 1$.

Furthermore, an approximate solution can be found for large values of the parameter $b^* = b/a$ (and small $\tilde{\alpha}^*$). However, we restrict our analysis to the more important physical solution (44).

The β -dependent solution (44) is valid for $\beta > \tilde{\beta}_c$, where

$$\tilde{\beta}_c \equiv -\frac{1}{\omega\sqrt{1-\tilde{\alpha}^*}} \ln \frac{A(1-\tilde{\alpha}^*)^{1/\gamma}}{1-(1-\tilde{\alpha}^*)^{1/\gamma}(\frac{A}{\gamma}-\frac{1}{1-\tilde{\alpha}^*})}.$$
 (45)

At $\omega\beta \gg 1$, the solutions of Eqs. (42) can be found perturbatively (for small ε) with given values of the parameters $(b-a)/(b+a)$ and $\tilde{\alpha}^*$. At $\varepsilon = 0$ [the solution (43)], the action (41) yields:

$$\begin{aligned} S &= \frac{\omega(b^2-a^2)}{(1-\tilde{\alpha}^*)^{3/2}} \operatorname{arcosh} \left[\frac{b-a}{b+a} \sinh \frac{\omega\beta\sqrt{1-\tilde{\alpha}^*}}{2} \right] \\ & - \frac{\omega^2\beta(b^2-a^2)}{2(1-\tilde{\alpha}^2)} + \frac{\omega(b+a)^2}{(1-\tilde{\alpha}^*)^{3/2}} \left[\coth \frac{\omega\beta\sqrt{1-\tilde{\alpha}^*}}{2} \right. \\ & \left. - \left(\sinh^{-2} \frac{\omega\beta\sqrt{1-\tilde{\alpha}^*}}{2} + \frac{(b-a)^2}{(b+a)^2} \right)^{1/2} \right]. \end{aligned}$$
 (46)

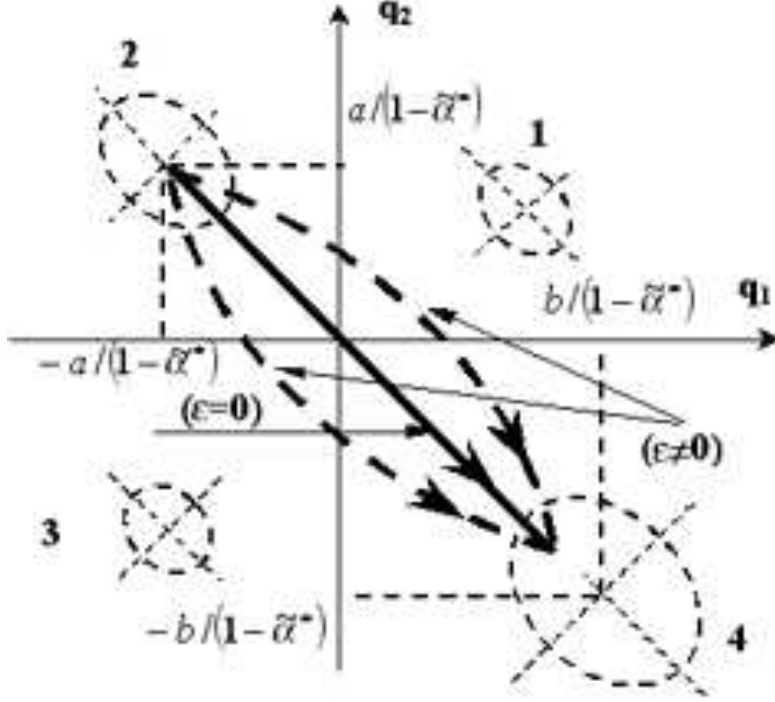


FIG. 13: Trajectories (the basic path characterized by $\varepsilon = 0$ and the split one is characterized by $\varepsilon \neq 0$) at $\omega\beta \gg 1$ of two antiparallel tunneling particles; (1)-(4) denote the projections of the minima of the potential energy surface $U_a(q_1, q_2)$ defined by Eq. (4).

For the symmetric potential ($a = b$) and $\varepsilon = 0$, we obtain that (see Fig. 11)

$$S = \frac{4\omega a^2}{(1 - \tilde{\alpha}^*)^{3/2}} \tanh \frac{\omega\beta\sqrt{1 - \tilde{\alpha}^*}}{4}. \quad (47)$$

We do not present here a cumbersome expression for $S_{\varepsilon \neq 0}$ which one can obtain by substituting the solutions τ and ε into Eq. (41). A simple analysis reveals that $S_{\varepsilon \neq 0} > S_{\varepsilon = 0}$ for $\beta > \tilde{\beta}_c$ and for relevant $\tilde{\alpha}^*$. Similarly to parallel transfer, the tunnel paths can be found from Eqs. (43) and (44). These trajectories on the (q_1, q_2) -plane are shown in Fig. 13.

As for parallel tunneling and at $\beta > \tilde{\beta}_c$, the pair-tunneling changes from a single to double trajectory regime. In contrast to the parallel tunneling, such a splitting occurs at any values of the parameters of the potential. At $\beta > \tilde{\beta}_c$, we have $S_{\varepsilon \neq 0} > S_{\varepsilon = 0}$ and, therefore, $S_{\varepsilon = 0}$ determines the tunneling rate. At $\beta < \tilde{\beta}_c$, the two degenerated trajectories are transformed into a single trajectory, $q_1 = -q_2$, corresponding to synchronous antiparallel transfer.

For single particle tunneling, there is only a single tunneling path (instanton) minimizing the action. Hence, there are two different types of trajectories for the pair of interacting particles. Namely, the main contribution to the instanton action is determined either by the single or by the double-degenerated paths depending on the value of β . We also point out that in the case of the parallel tunneling, the particles do not simultaneously pass the top points of the barrier, $\tau_1 \neq \tau_2$. This means that the tunneling transfer is asynchronous.

At small values of the interaction parameter α^* [see Eq. (37)] and at temperatures such that $\beta < \beta_c$ [see Eq. (38)], there is no splitting of a single path ($q_1 = q_2$). Therefore, the particles pass the top of the barriers at the same instants ($\tau_1 = \tau_2$). Consequently, the transfer of the particles is synchronous. The temperature dependence for the antiparallel transfer action is plotted in Fig. 14 at various $\tilde{\alpha}^*$.

The type of the interaction given by Eqs. (2)-(5) is such that it does not affect the motion along the "center of mass" coordinate, $q_1 = q_2$. For this reason, the Euclidean action is independent of the interaction parameter as for parallel transfer. Since the state of the interacting system characterized by a maximal value of the relative coordinate, $q_1 = -q_2$, is preferable (as it provides the lower action), it becomes clear that the instanton action decreases with

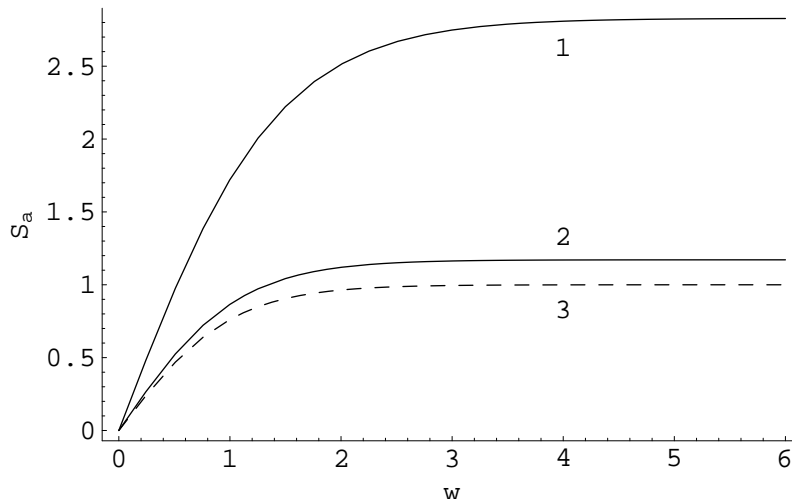


FIG. 14: Instanton action for antiparallel tunneling ($\varepsilon = 0$, $a = b$) as a function of an inverse temperature at the two different values of the interaction parameter; $S_a = S/(4\omega a^2)$, $w = \omega\beta/4$; (1) $\tilde{\alpha}^* = 0.5$; (2) $\tilde{\alpha}^* = 0.1$; (3) a dashed line corresponds to the action (40) for the parallel transition ($\varepsilon = 0$, $a = b$).

the interaction parameter in the parallel transfer along the degenerated tunnel trajectories, and increases with the interaction parameter for the antiparallel tunneling.

For antiparallel tunneling, synchronous transfer ($\tau_1 = \tau_2$) takes place, while asynchronous transfer is forbidden due to the greater contribution to the Euclidean action (see Fig. 14).

The validity condition for weakly interacting instanton-antiinstanton pairs, in the adiabatic approximation, was discussed in Ref. [27].

The numerical analysis of transcendental equation (42) reveals interesting features for a transition region between the tunneling regimes, i.e., a fine structure near the first bifurcation point for the antiparallel transfer. The numerical results are presented in Fig. 15. We found that, in addition to the first bifurcation point characterized by the two solutions (Fig. 15a), there exist additional bifurcation points at lower temperatures, i.e., the four pairs (Fig. 15b), the six pairs (Fig. 15c), and there are even twelve pairs of additional solutions at $\beta^* = 19.2009$ ($\alpha^* = 0.05$), etc. We refer to this phenomenon as multiplication of bifurcations or a *cascade of bifurcations*. Such an effect resembles a scenario of transition to chaos.

Although the synchronous regime is preferred due to the minimal instanton action, in a certain temperature range its value is comparable with those of corresponding to the cascade solutions. As a result, *quantum fluctuations* of a nonregular character occur in contrast to the parallel transfer. The antiparallel tunneling is, thus, characterized by the instability of the transition due to the synchronous to asynchronous behavior. Such instabilities are similar to continuous second-order phase transition, while the parallel tunneling is viewed as a step process similar to phase transition of a first order (see Fig. 10). The dependencies shown in Figs. 11 and 12, $\beta_c(\alpha)$ and $\alpha_c(\beta)$, for the antiparallel transfer are found to be of the same character as those of the parallel transfer.

In summary, our investigation reveals a quite complicated fine structure of the transition for parallel and antiparallel tunneling of two particles with different degenerate trajectories leading to the bifurcation cascade.

VII. EFFECT OF A PROMOTING MODE

In this section, we study the effect of a heat bath on tunneling transition of two interacting particles. In many tunneling reactions, interaction with a vibrational subsystem can often be approximated by interaction with a single vibrational mode (a so-called promoting mode). As it follows from Eq. (19), a heat bath affects only the dynamics of the center of mass ($q_1 = q_2$). Therefore, in the case of an antiparallel motion, the medium does not affect the rate constant, while for parallel tunneling it essentially contributes to the transfer rate. For both parallel and antiparallel transfer, bilinear interaction of the particles with a single oscillator can make a qualitative change in the character of tunneling.

At small values of the interaction parameter between the two tunneling particles dissipative effects become important

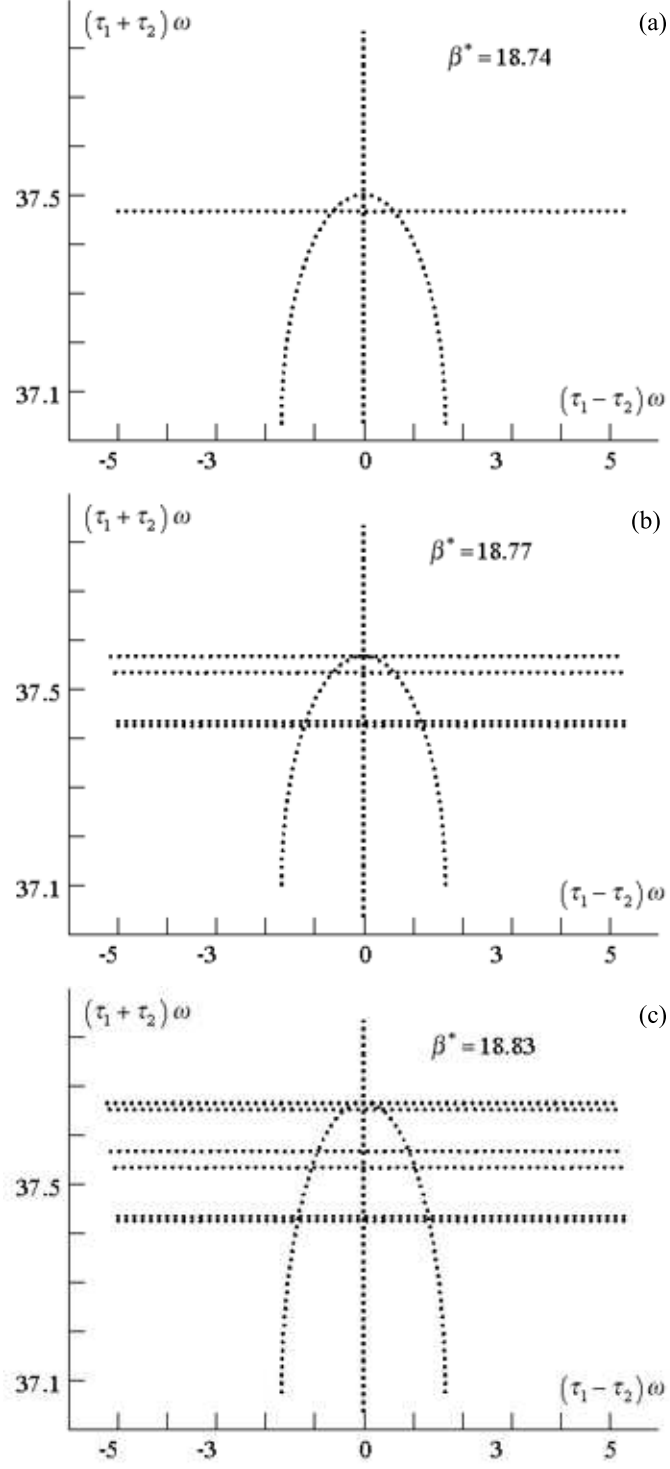


FIG. 15: Numerical solutions of transcendental equation (42). In addition to the studied solution $\tau_1 = \tau_2$, with respect to β , there are the additional solutions, $\tau_1 \neq \tau_2$, shown in panels (a), (b) and (c), that correspond to one, four, and six (pairs) additional solutions, respectively.

[27]. In two dimensions the dissipative effects are more pronounced for parallel rather than antiparallel tunneling. The latter increases with temperature with a considerable contribution to the prefactor. In the present work, we are interested in the tunneling rate assuming only exponential evolution of the transition probability. However, nonexponential evolution can occur in a nonequilibrium environment [38, 39, 40, 41]. Such a case is not discussed here. Accordingly, a reservoir is assumed to be in thermodynamic equilibrium, i.e., the tunneling transition is rather slow compared to the thermodynamic relaxation. Thus, we assume that dissipation affects the value of instanton action only.

For the case of the antiparallel tunnel transfer, the action (32) can be calculated with the following vibronic Green's function:

$$D(\nu_n) = -\frac{C^2}{\nu_n^2 + \omega_L^2}, \quad (48)$$

where ω_L is the frequency of the vibrational mode. After some tedious calculations, one obtains the following expression for the instanton action (32):

$$\begin{aligned} S = & \frac{2\omega^4(a^2 - b^2)\tau_0}{\Omega_0^2} - \frac{2\omega^4(a+b)^2}{\beta} \\ & \times \left\{ -\frac{\beta \sinh(\Omega_0(\beta/2 - \tau_0)) \sinh(\Omega_0\tau_0)}{2\Omega_0^3 \sinh(\Omega_0\beta/2)} \right. \\ & + \sum_{i=1}^2 \frac{\beta(\Omega_i^2 - \omega_L^2) \cosh(\Omega_i(\beta/2 - \tau_0)) \cosh(\Omega_i\tau_0)}{(-1)^i 2\Omega_i^3 (\Omega_1^2 - \Omega_2^2) \sinh(\Omega_i\beta/2)} \\ & + \frac{\beta\varepsilon}{4(\omega^2 - 2C^2/\omega_L^2)} - \frac{\beta\varepsilon}{4\Omega_0^2} + \frac{\beta \sinh(\varepsilon\Omega_0)}{4\Omega_0^3} \\ & + \sum_{i=1}^2 \frac{\beta(\Omega_i^2 - \omega_L^2) \sinh(\varepsilon\Omega_i)}{(-1)^i 4\Omega_i^3 (\Omega_1^2 - \Omega_2^2)} + \frac{\beta \cosh(\varepsilon\Omega_0)}{4\Omega_0^3 \sinh(\beta\Omega_0/2)} \\ & \times [\cosh(\Omega_0(\beta/2 - 2\tau_0)) - \cosh(\Omega_0\beta/2)] \\ & - \sum_{i=1}^2 \frac{\beta(\Omega_i^2 - \omega_L^2) \cosh(\varepsilon\Omega_i)}{(-1)^i 4\Omega_i^3 (\Omega_1^2 - \Omega_2^2) \sinh(\beta\Omega_i/2)} \\ & \left. \times [\cosh(\Omega_i(\beta/2 - 2\tau_0)) + \cosh(\Omega_i\beta/2)] \right\}. \quad (49) \end{aligned}$$

Here, we have introduced the following notation:

$$\begin{aligned} \Omega_0^2 &= \omega^2 - \alpha^2, \quad \Omega_1^2 = \frac{1}{2}(\omega^2 + \omega_L^2 + \sqrt{(\omega^2 - \omega_L^2)^2 + 8C^2}), \\ \Omega_2^2 &= \frac{1}{2}(\omega^2 + \omega_L^2 - \sqrt{(\omega^2 - \omega_L^2)^2 + 8C^2}). \end{aligned}$$

For the parallel tunneling transition, a corresponding action can be found in a similar way. The action (34) as a function of the parameters $\varepsilon^* = \tau_1 - \tau_2$ and $\tau^* = (\tau_1 + \tau_2)/2$, with the vibronic frequency ω_L and coupling constant C , yields (see also Ref. [27]):

$$\begin{aligned} S = & (a+b)(3a-b)\omega^2\tau^* - \frac{\omega^4(a+b)^2\varepsilon^*}{2(\omega^2 - 2\alpha)} - \frac{4\omega^2(a+b)^2\tau^{*2}}{\beta} \\ & - \frac{4\omega^4(a+b)^2\varepsilon^{*2}}{(\omega^2 - 2\alpha)\beta} - \frac{\omega^2(a+b)^2}{2\tilde{\gamma}} \sum_{i=1}^2 \frac{(-1)^i(\omega^2 - x_{3-i})}{\sqrt{x_i}} \\ & \times \left[\coth\left(\frac{\beta\sqrt{x_i}}{2}\right) - \sinh^{-1}\left(\frac{\beta\sqrt{x_i}}{2}\right) \left(\cosh\left[\left(\frac{\beta}{2} - 2\tau^*\right)\sqrt{x_i}\right] \right. \right. \\ & \left. \left. - \cosh\left[\left(\frac{\beta}{2} - \varepsilon^*\right)\sqrt{x_i}\right] + \frac{1}{2}\cosh\left[\left(\frac{\beta}{2} - 2\tau^* - \varepsilon^*\right)\sqrt{x_i}\right] \right. \right. \\ & \left. \left. + \frac{1}{2}\cosh\left[\left(\frac{\beta}{2} - 2\tau^* + \varepsilon^*\right)\sqrt{x_i}\right] \right) \right] + \frac{\omega^4(a+b)^2}{2(\omega^2 - 2\alpha)^{3/2}} \\ & \times \left[-\coth\left(\frac{\beta}{2}\sqrt{\omega^2 - 2\alpha}\right) + \sinh^{-1}\left(\frac{\beta}{2}\sqrt{\omega^2 - 2\alpha}\right) \right] \end{aligned}$$

$$\begin{aligned}
& \left(-\cosh\left[\left(\frac{\beta}{2} - 2\tau^*\right)\sqrt{\omega^2 - 2\alpha}\right] + \cosh\left[\left(\frac{\beta}{2} - \varepsilon^*\right)\sqrt{\omega^2 - 2\alpha}\right] \right. \\
& \quad \left. + \frac{1}{2}\cosh\left[\left(\frac{\beta}{2} - 2\tau^* - \varepsilon^*\right)\sqrt{\omega^2 - 2\alpha}\right] \right. \\
& \quad \left. + \frac{1}{2}\cosh\left[\left(\frac{\beta}{2} - 2\tau^* + \varepsilon^*\right)\sqrt{\omega^2 - 2\alpha}\right] \right) \Bigg]. \tag{50}
\end{aligned}$$

Here, we have denoted

$$\begin{aligned}
x_{1,2} &= \frac{1}{2}(\omega^2 + \omega_L^2 + \frac{C^2}{\omega_L^2}) \mp \frac{1}{2}\tilde{\gamma}, \\
\tilde{\gamma} &= \sqrt{(\omega^2 + \omega_L^2 + \frac{C^2}{\omega_L^2})^2 - 4\omega^2\omega_L^2}.
\end{aligned}$$

For particular values of the interaction constant α and in the absence of interaction with the oscillator bath, the critical temperature T_c (at which the synchronous and asynchronous tunnel regimes interchange) is found from Eqs. (38) and (45). These equations can be generalized to non-zero interaction with the promoting mode. Typically, the critical temperature is found to be in the range from 10 K to 400 K . In glasses, T_c can be very small while for chemical reactions it can be rather large. Additionally, T_c depends on the mean distance between the particles and, therefore, on their concentration.

Quantum tunneling is important [28] when $k_B T_c / (\hbar\omega) \leq 1$. Therefore, the symmetry breaking effects can take place at relatively high temperatures depending on the "frequency" of a barrier. For example, for porphyrins the critical temperature T_c is estimated to be about 200 K .

VIII. CONCLUSIONS

In the single instanton approximation, we have calculated the Euclidean action (19) for the models characterized by the different adiabatic potential energy surfaces, (3), (4) and (5), and made a detailed comparative analysis of the tunneling rate for two interacting particles moving in parallel or antiparallel within a dissipative environment. We have also assumed exponential evolution of the transition probability [27, 38, 39, 40, 41].

We have shown that the change in a tunneling regime from synchronous to asynchronous transfer for parallel transition occurs as a step process, similar to phase transition of a first order, while for the antiparallel transfer it resembles second order phase transition.

We have explained the effect of a *cleavage* in the experimentally observed [24, 25, 26, 33] temperature dependence of the reaction rate for two tunneling particles. It has been shown that the effect of symmetry breaking is stable for the parallel and unstable for the antiparallel transfer, as it is observed experimentally for some porphyrin systems [24, 25, 26, 33]. We have found a complicated fine structure in the bifurcation region due to the *quantum fluctuations* for the parallel two-dimensional tunneling. For the antiparallel tunneling, the contribution of four, six, twelve, etc., pairs of trajectory becomes important resembling the transition to *chaos*.

Additionally, we have studied interaction of two particles with phonons. Such coupling essentially modifies the antiparallel and parallel transitions in different ways. As it follows from Eq. (19), the interaction with the reservoir does not change the dynamics of the center of mass for the antiparallel motion, while it makes a significant contribution to the transfer rate for the parallel transfer. Finally, Eq. (38) determines the validity condition for temperatures beyond of which stable two-dimensional synchronous tunneling correlations of all the kinds occur.

The authors would like to thank A. I. Larkin and B. I. Ivlev for the stimulating interest in this work.

-
- [1] R. Meyer and R. R. Ernst, J. Chem. Phys. **86**, 784 (1987).
 - [2] A. O. Caldeira, A. J. Leggett, Phys. Rev. Lett. **46**, 211 (1981).
 - [3] I. Affleck, Phys. Rev. Lett. **46**, 388 (1981).
 - [4] P. G. Wolynes, Phys. Rev. Lett. **47**, 968 (1981).
 - [5] A. I. Larkin and Yu. N. Ovchinnikov, Pis'ma v Zh. Eksp. Teor. Fiz. **37**, 322 (1983).
 - [6] B. I. Ivlev and Yu. N. Ovchinnikov, Zh. Eksp. Teor. Fiz. **93**, 668 (1987).
 - [7] H. Grabert and U. Weiss, Z. Phys. B **56**, 171 (1984).

- [8] A.O. Caldeira and A.J. Leggett, Ann. of Phys. **149**, 374 (1983); A. J. Leggett, S. Chakravarty, A. J. Dorsey, M. P. A. Fisher, A. Garg, and W. Zwegler, Rev. Mod. Phys. **59**, 1 (1987).
- [9] V. I. Mel'nikov, Zh. Eksp. Teor. Fiz. **87**, 663 (1984).
- [10] H. Dekker, Phys. Rep. **80**, 1 (1981).
- [11] A. Schmid, Ann. of Phys. **170**, 333 (1986).
- [12] A. D. Zaikin and S. V. Panyukov, Zh. Eksp. Teor. Fiz. **89**, 1890 (1985).
- [13] Yu. Kagan and N. V. Prokof'ev, Pis'ma v Zh. Eksp. Teor. Fiz. **43**, 434 (1986).
- [14] H. Grabert and U. Weiss, Phys. Rev. Lett. **54**, 1605 (1985).
- [15] M. Yu. Sumetskii, Zh. Eksp. Teor. Fiz. **89**, 618 (1985).
- [16] Yu. N. Ovchinnikov, Zh. Eksp. Teor. Fiz. **94**, 365 (1988).
- [17] B. I. Ivlev, Zh. Eksp. Teor. Fiz. **94**, 333 (1988).
- [18] U. Weiss, *Quantum Dissipative Systems* (World Scientific, Singapore, 1993).
- [19] H. Grabert, P. Schramm, and G.-L. Ingold, Phys. Reps. **168**, 115 (1988).
- [20] L. Gammaitoni, P. Hänggi, and P. Jung, Rev. Mod. Phys. **70**, 223 (1998).
- [21] K. Yamamoto, Progr. Theor. Phys. **96**, 1147 (1996).
- [22] V. A. Benderskii and D. E. Makarov, Phys. Reps. **233**, 197 (1993).
- [23] J. Ankerhold and H. Grabert, Phys. Rev. E **61**, 3450 (2000); Europhys. Lett. **47**, 285 (1999).
- [24] Z. Smedarchina, W. Siebrand, and T. A. Wildman, Chem. Phys. Lett. **143**, 395 (1988).
- [25] Z. Smedarchina, W. Siebrand, and F. Zerbetto, Chem. Phys. **136**, 285 (1989).
- [26] K. Tokumura, Y. Watanabe, and M. Itoh, J. Phys. Chem. **90**, 2362 (1986).
- [27] Yu. I. Dakhnovskii, A. A. Ovchinnikov, and M. B. Semenov, Zh. Eksp. Teor. Fiz. **92**, 955 (1987).
- [28] Yu. I. Dakhnovskii and M. B. Semenov, J. Chem. Phys. **91**, 7606 (1989).
- [29] Yu. I. Dakhnovskii, A. A. Ovchinnikov, and M. B. Semenov, Hadronic J. **25**, 303 (2002).
- [30] V. A. Benderskii, E. V. Vetoshkin, and E. I. Kats, Zh. Eksp. Teor. Fiz. **122**, 746 (2002); cond-mat/0303275 (2003); V. A. Benderskii, E. V. Vetoshkin, E. I. Kats, and H. P. Trommsdorff, cond-mat/0209030 (2002).
- [31] H. Frauenfelder, in *Physics of Biological Systems: From molecules to species*, edited by H. Flyvbjerg, J. Hertz, M. H. Jensen, O. G. Mouritsen, and K. Sneppen (Springer, Berlin, 1997), p. 29.
- [32] K. Tagami, M. Tsukada, T. Matsumoto, and T. Kawai, Phys. Rev. B **67**, 245324 (2003).
- [33] V. M. Mamaev and V. V. Gorchakov, *Foundations of chemical dynamics: the potential energy surfaces and tunnel dynamics* (DGU, Vladivostok, 1988).
- [34] D. J. W. Geldart and D. Neilson, cond-mat/0303008 (2003).
- [35] J. Hennig, H. H. Limbach, J. Chem. Soc. Faraday Trans. II. **75**, 752 (1979); H. H. Limbach, J. Hennig, D. Gerritzen, and H. Rumpel, Faraday Discussions Chem. Soc. **74**, 229 (1982); P. Stibbs and M. E. Mosely, J. Chem. Soc. Faraday Trans. II. **76**, 729 (1980).
- [36] L. L. Gladkov and K.N. Solov'yov, Spectrochem. Acta., **41** A, 1437 (1985).
- [37] Sebastian et al., Chem. Phys. **61**, 125 (1981); **75**, 105 (1983); Bonnds et al., Chem. Phys. **63**, 303 (1981); **95**, 197 (1985); Petelenz et al., Chem. Phys. **111**, 209 (1987); **119**, 25 (1988); **131**, 409 (1989); **133**, 199 (1989); Chem. Phys. Lett., **133**, 157 (1987); **147**, 430 (1988).
- [38] M. Hornbach and Yu. Dakhnovskii, J. Chem. Phys. **111**, 5073 (1999).
- [39] Yu. Dakhnovskii, J. Chem. Phys. **111**, 5418 (1999).
- [40] D. G. Evans, A. Nitzan, and M. A. Ratner, J. Chem. Phys. **108**, 6387 (1998).
- [41] Yu. Dakhnovskii, V. Lubchenko, and P. Wolynes, J. Chem. Phys. **104**, 1875 (1996).